The Hippo transducer TAZ interacts with the SWI/SNF complex to regulate breast epithelial lineage commitment

Adam Skibinski[1,2], **Jerrica L. Breindel**[1,2], **Aleix Prat**[3], **Patricia Galván**[3], **Elizabeth Smith**[1], **Andreas Rolfs**[4], **Piyush B. Gupta**[4,5], **Joshua LaBaer**[6], and **Charlotte Kuperwasser**[1,2]

[1]Department of Developmental, Chemical, and Molecular Biology, Tufts University, 145 Harrison Ave., Boston, MA 02111

[2]Molecular Oncology Research Institute, Tufts Medical Center, 800 Washington St., Boston, MA 02111

[3]Translational Genomics Group, Vall d'Hebron Institute of Oncology, Passeig de la Vall d'Hebron 119-129, Barcelona, ES 08035

[4]Department of Biology, Massachusetts Institute of Technology, Cambridge, MA 02139, USA

[5]Whitehead Institute for Biomedical Research, Nine Cambridge Center, Cambridge MA, 02142

[6]Center for Personalized Diagnostics, Biodesign Institute, Arizona State University, 727 E. Tyler St., Tempe, AZ 85287

Abstract

Lineage-committed cells of many tissues exhibit substantial plasticity in contexts such as wound healing and tumorigenesis, but the regulation of this process is not well understood. Here, we identified the Hippo transducer *WWTR1/TAZ* in a screen of transcription factors able to prompt lineage switching of mammary epithelial cells. Forced expression of TAZ in luminal cells induces them to adopt basal characteristics, and depletion of TAZ in basal/myoepithelial cells leads to luminal differentiation. In human and mouse tissues, TAZ is active only in basal cells and is critical for basal cell maintenance during homeostasis. Accordingly, loss of TAZ affects mammary gland development, leading to an imbalance of luminal and basal populations as well as branching defects. Mechanistically, TAZ interacts with components of the SWI/SNF complex to modulate lineage-specific gene expression. Collectively, these findings uncover a new role for Hippo signaling in the determination of lineage identity through recruitment of chromatin remodeling complexes.

#Correspondence may be addressed to: Charlotte Kuperwasser, Department of Developmental, Molecular and Chemical Biology, Tufts University School of Medicine, 800 Washington St, Box 5609, Boston, MA 02111, Phone: (617) 636-2364; Fax: (617) 636-6217, Charlotte.Kuperwasser@tufts.edu.

Keywords

WWTR1/TAZ; Hippo pathway; cellular plasticity; SWI/SNF; differentiation; mammary gland; lineage commitment

Introduction

Cellular differentiation can no longer be considered a permanent or unidirectional process, given the mounting examples where cells are able to change their identity in response to a variety of physiologic, pathologic, or experimental stimuli (Galliot and Ghila, 2010). The strongest evidence for such phenomena comes from recent lineage-tracing studies in diverse settings such as the lung (Tata et al., 2013), pancreas (Zhou et al., 2008), and hair follicle (Rompolas et al., 2013), in which the fates of differentiated cells and their progeny were definitively mapped with genetic markers. A common theme in these examples is that in response to tissue injury, *ex vivo* culture, or oncogenic transformation, lineage-committed cells and/or their progeny exhibit "lineage infidelity" and adopt alternate cell fates. The context-dependent nature of such plasticity strongly implies regulation; however, in most cases, the important players have not been identified.

Cells of the mammary epithelium also exhibit context-dependent plasticity. They are comprised of two major cell populations, luminal and basal/myoepithelial (ME), which are distinguishable in terms of their anatomic location, function, and ontogeny (Visvader, 2009). Luminal cells line the lumens of ducts and alveoli and are responsible for milk production, while basal/ME cells contact the basement membrane and contract to pump milk through the ducts. Both populations originate from a common *KRT14*-expressing mammary stem cell (MaSC) during embryonic development (Spike et al., 2012; Tsai et al., 1996; Visvader and Lindeman, 2006) but the existence and significance of MaSCs in adult tissues remains contentious. Genetic lineage tracing studies from different groups have produced irreconcilable data that either demonstrate or refute the presence of MaSCs in adult tissues (Rios et al., 2014; (van Keymeulen et al. 2011, Van Amerongen et al., 2012). On the other hand, regardless of the marker used for in vivo labeling, no lineage tracing studies have identified bipotent luminal cells *in situ*, indicating that all luminal cells appear to be lineage-restricted during normal development (van Keymeulen et al., 2011).

However, basal and luminal lineage barriers clearly break down in certain non-physiologic settings. It is well known that murine basal cells have the capacity to generate an entire functional mammary epithelial tree when transplanted into the cleared fat pat of a recipient mouse (Kordon and Smith, 1998; Shackleton et al., 2006), even when it can be demonstrated by lineage tracing that the transplanted cells do not exhibit bipotent differentiation potential during normal development (Van Amerongen et al., 2012). While luminal cells generally lack this potential, *ex vivo* culture of luminal human mammary epithelial cells can induce them to adopt stem-like or bipotent features (Keller et al., 2012; Chaffer et al., 2011; Pechoux et al., 1999). In addition, luminal cells are the likely cells-of-origin for basal-like breast tumors, suggesting that they also acquire plasticity during tumorigenesis (Keller et al., 2012; Proia et al. 2011, Molyneux et al., 2010).

What allows lineage-committed MECs to become bi-potent in these settings? Transcription factors (TFs) are likely candidates, since they are master orchestrators of the gene expression programs that define specific differentiation states. Thus, we sought to determine whether committed luminal cells could be induced to acquire features of basal/ME cells by the activity of a single transcription factor. We developed a gain-of-function screen in which TFs were expressed in luminal epithelial cells, and identified candidates able to induce a basal/ME-like phenotype. Using this approach, we identified the Hippo transducer *WWTR1/TAZ* as a regulator of the basal/ME progenitor phenotype in the mammary gland. We demonstrate that modulation of TAZ is sufficient to effect changes in differentiation state, and that it directly associates with SWI/SNF chromatin-remodeling complexes to both repress the expression of luminal-specific genes and activate basal-specific genes.

Results

Identification of TAZ in a gain-of-function screen of epithelial lineage plasticity

Previously, we reported that highly pure populations of EpCAM+ luminal and CD10+ basal/ME cells can be isolated from the bulk population of cells derived from discarded breast reduction tissues (Keller et al., 2012). Cells isolated this way exhibit different colony-forming potential *in vitro*. CD10+ basal cells readily form adherent colonies on tissue culture substrates and rapidly acquire a bi-potent differentiation state, expressing both luminal and basal cytokeratins. In contrast, EpCAM+ luminal cells rarely attach to plastic substrates, reflecting the minimal contact between luminal cells and the extracellular matrix (ECM) *in vivo*. Instead, they float in suspension as spherical colonies and retain their luminal characteristics. Thus, we endeavored to identify potential regulators of epithelial plasticity by screening for TFs that would prompt luminal cells to adopt an adherent phenotype.

A pooled lentiviral cDNA library consisting of ~1000 human TFs was generated for this purpose (Table S1). We then employed FACS to isolate EpCAM+ luminal cells from freshly dissociated reduction mammoplasty tissue, and transduced the cells either with the pooled lentiviral library or with an empty-vector control lentivirus (Figure 1A). Infected cells were seeded under adherent conditions and allowed to form colonies, while the non-adherent cells were discarded. To identify the factors promoting luminal cell adherence, transduced TF cDNAs were recovered from genomic DNA by PCR, followed by high-throughput sequencing of the PCR amplicons. An enrichment score for each TF was calculated by dividing the number of reads for each TF in the screened cells by that of transduced (but unscreened) control cells.

Using this approach we identified 52 TFs with greater than two-fold enrichment in the screened cells relative to control cells (Figures 1B, 1C). We noted that six TF hits (HOXA5, HOXA9, ID1, ID2, ID3, and SNAI1) have been previously implicated in either basal/ME epithelial differentiation or EMT, and four additional hits (BTBD1, LIMS1, KLHDC5, HOXC4) have also been recently reported to be preferentially expressed in human mammary basal/stem cells (MaSC), a testament to the validity of the approach (Lim et al., 2010) (Figure 1C). Indeed, gene set enrichment analysis of the screen "hits" revealed enrichment in previously published gene expression profiles of sorted basal/ME cells,

further demonstrating that adherent colony formation is indeed a valid surrogate marker for the basal/ME cell phenotype (Fig 1D).

Among the remaining 42 novel hits we identified *WWTR1*, a transducer of Hippo signaling (commonly referred to as TAZ, 7.38-fold enriched). TAZ and its paralog YAP are transcriptional co-activators that lack a DNA-binding domain, but regulate self-renewal and differentiation of stem cells in many cell tissue types via direct interaction with sequence-specific DNA-binding proteins, such as the TEAD family of transcription factors (Pan, 2010). We were intrigued by previous studies which demonstrated that TAZ overexpression can trigger proliferation and induce EMT-like changes in epithelial cells (Lei et al., 2008). Basal/ME cells share many features with mesenchymal cells, such as a lack of apicobasal polarity, limited intercellular contacts, and high vimentin expression (Prat et al., 2013; Sarrió et al., 2008) . We therefore hypothesized that TAZ might also be able to impart such properties to luminal MECs.

To validate the ability of TAZ to promote adherent colony formation, freshly dissociated MECs were FACS-sorted and transduced with lentivirus containing TAZ cDNA alone. Consistent with the primary screen, TAZ overexpression led to a five- to ten-fold increase in the number of adherent colonies observed after plating of freshly dissociated EpCAM+ luminal cells (Figure 1E). Furthermore, when TAZ was overexpressed in unsorted cells, we observed a measurable increase in the formation of bipotent KRT14+/KRT18+ colonies as well as an increase in K14+ myoepithelial colonies (Figure 1F) compared with control cells. We also seeded the same cells in 3D collagen/matrigel cultures. We have previously shown that when grown in collagen/matrigel, CD10+ basal/ME cells preferentially formed elongated ductal structures or flat colonies, whereas EpCAM+ luminal cells formed round acinar structures (Keller et al., 2012). Forced TAZ expression led to a decrease in round colonies with a corresponding increase in flat colonies (Figure 1G); thus, TAZ-infected cells behaved similarly to primary basal cells. We conclude that in primary MECs, TAZ expression is sufficient for committed luminal cells to adopt features of basal/ME cells.

TAZ controls mammary epithelial differentiation state

Based on the above findings, we hypothesized that TAZ might act to promote linage switching by repressing luminal-specific gene expression and/or activating basal/ME-specific gene expression, resulting in basal/ME differentiation. To test this, we utilized MCF10A and MCF10F cell lines, which are non-tumorigenic, spontaneously immortalized mammary cell lines derived from the same donor. MCF10F and MCF10A cells were derived from disease-free breast tissue; MCF10F cells were generated from free-floating cells in the primary culture and are heterogeneous, containing stable subpopulations of luminal-like and basal-like cells (Figure 2D). In contrast, MCF10A cells were derived from the adherent cells and homogeneously exhibit a predominantly basal-like phenotype with low expression of luminal markers compared to MCF10F (Soule et al., 1990 and Figure S1A, red bars). Examination of endogenous TAZ expression levels in the MCF10 system revealed that basal-like MCF10A cells expressed higher levels of TAZ relative to the more luminal-like MCF10F cells (Figure S1A, gray bar). Therefore, to examine how TAZ may promote lineage switching, we expressed TAZ cDNA in MCF10F cells or inhibited TAZ in MCF10A

cells using shRNAs, and asked whether TAZ modulation could influence differentiation state.

When TAZ was overexpressed in MCF10F cells, they adopted a distinct elongated morphology, forming looser colonies and exhibiting a striking lack of cell-cell contacts (Figures 2A). When grown in 3D collagen cultures, MCF10F-TAZ cells generated significant fewer round colonies than control cells, and exhibited a trend toward increased ductal morphogenesis, similar to primary MECs (Figure 2B). Furthermore, lineage-specific marker and gene expression analysis of MCF10F-TAZ cells also revealed changes in their differentiation potential. We noticed that MCF10F cells were heterogeneous. Luminal and basal subpopulations of MCF10F cells could be resolved by flow cytometry using a combination of EpCAM and CD44 expression (Figure 2C and Figure S1B), and FACS-purified cells from these populations also expressed additional luminal- and basal-specific lineage markers (Figure S1C) and exhibited distinct morphologies (Figure S1D). Interestingly, TAZ overexpression in MCF10F cells caused an expansion of the basal subpopulation relative to the luminal subpopulation, suggesting that TAZ may enhance the conversion of luminal MCF10F cells into basal MCF10F cells (Figure 2D), and replacing wild-type TAZ cDNA with a constitutively active mutant TAZ (S89A) dramatically amplified this effect.

The shift toward a basal immunophenotype was also associated with reduced expression of luminal markers such as *MUC1, CDH1, EpCAM*, and *GATA3* (Figure 2E). Expression of the TAZ-S89A mutant also led to similar gene expression changes (Figure S1E). Although luminal epithelial markers such as *EpCAM* and *CDH1* were significantly reduced in MCF10F-TAZ cells, the expression of cytokeratins remained high, suggesting that the cells had not undergone EMT. However, because mRNA levels of basal markers did not increase significantly (Figure 2E), the EpCAM-/CD44+ cells that expanded in response to TAZ most likely represent an intermediate state, and additional factors may be required along with TAZ to fully specify basal differentiation.

As TAZ expression was sufficient to repress the luminal phenotype, we next wondered whether TAZ was also required in basal MCF10A cells to maintain their differentiation state. Therefore, we used lentivirus to deliver shRNAs against *TAZ* to MCF10A cultures, depleting TAZ protein levels to ∼25% that of control cells (shScram vs shTAZ, Figure 2F-K).

MCF10A-shTAZ cultures grew more slowly than shScram cells (Figure 2H) and generated fewer mammospheres under non-adherent culture conditions (Figure 2I) suggesting a decrease in proliferative potential and/or progenitor activity. Intriguingly, a significant proportion of shTAZ cells detached from the plastic substrate and floated as nonadherent cells in the growth medium (Figure 2F, arrows), reminiscent of the phenotype of primary luminal breast epithelial cells. When grown at low density in a 50% mixture of collagen I and Matrigel, the propensity of shTAZ cells to generate ductal structures was markedly reduced; adherent shTAZ cells formed 80% fewer ductal colonies than control cells (Figure 2J). However, floating shTAZ cells did not expand in number in either 2D or 3D adherent

conditions or as non-adherent mammospheres, suggesting a near-complete lack of proliferative potential in these cells (not shown).

We performed gene expression analysis of various lineage markers of basal and luminal differentiation on adherent and floating shTAZ cells. We used global gene expression data from Lim et al. (2010) to identify marker genes associated with basal/MaSC, luminal progenitor, or mature luminal differentiation state and analyzed the expression of these genes in adherent vs. floating cells lacking TAZ using qPCR as well as the nCounter platform (Figure 2K and Figure S1F-G). Both populations of shTAZ cells (floating and adherent) showed a strong decrease in proliferation-associated gene expression compared with control cells, consistent with the decrease in proliferative capacity of shTAZ cells (Figure S1F, right). Adherent shTAZ cells displayed an increase in several markers of luminal differentiation, such as *CD24, MUC1* and *CLDN4*, and in particular displayed up-regulation of markers of luminal progenitor cells (e.g. *KRT6B, CD14*, and *ALDH1A3*, Figure S1G). Paradoxically, these cells also exhibited upregulation of *KRT14*, although *KRT14* is also expressed in a subset of luminal cells in the human mammary gland (Santagata et al., 2014). Non-adherent shTAZ cells showed very strong expression of the same genes and also expressed more mature luminal transcripts including *ESR1* and *PGR*, which are typically only expressed in a subset of mature non-proliferating luminal cells. We confirmed the expression of ERα protein in floating shTAZ cells by Western blot (Figure S1H).

Because YAP and TAZ often exhibit functional redundancy, we also asked whether YAP is also able to repress luminal differentiation. Unlike TAZ, YAP knockdown did not lead to changes in cellular morphology or to loss of adhesion (Figure S1I). While YAP knockdown in MCF10A cells led to repression of the well-known YAP/TAZ target gene *CTGF*, these cells did not exhibit the same transcriptional changes in lineage markers as shTAZ cells and in fact YAP knockdown appeared to result in opposite changes in many lineage markers (Figure S1J). Therefore, repression of luminal differentiation is a unique function of TAZ.

Collectively, the data presented in Figure 2 suggest that TAZ can dynamically modulate differentiation state in MECs. It is both sufficient to induce repression of lineage-specific genes in luminal cells and required to maintain their repression in basal cells; hence, luminal cells transition to a basal cell fate when TAZ is overexpressed, and basal cells undergo luminal differentiation when TAZ is depleted.

Hippo signaling restricts TAZ to basal/ME cells

To determine whether TAZ functions in a lineage-specific manner in basal cells *in vivo*, we examined the distribution of TAZ, its upstream regulators, and its transcriptional targets in the mammary epithelium.

TAZ and its paralog YAP are regulated by the Hippo pathway (Zhao et al., 2011). In response to Hippo signaling, TAZ is phosphorylated by LATS1/2 kinases, resulting in its inactivation by either cytoplasmic retention, and/or ubiquitin-mediated destruction by the β-TRCP complex. Therefore, to examine whether the nuclear localization of TAZ in basal cells was associated with differences in Hippo signaling, purified EpCAM+ luminal and CD10+ basal/ME cells were isolated from breast tissues using immunomagnetic beads

(Figure 3A-B), and the level of TAZ and phospho-LATS1 were assessed by Western blotting (Figure 3C).

Interestingly, strong activation of the Hippo pathway was detected in luminal cells as evidenced by a high level of phospho-LATS1 expression in this population (Figure 3C). Yet surprisingly, total protein levels of TAZ were not different in luminal cells vs. basal cells, nor were TAZ mRNA levels significantly different between the two subpopulations (Figure S2A and S2B). However, immunostaining of normal breast tissues with an antibody reactive to both YAP and TAZ revealed a clear difference in the localization of YAP/TAZ (Figure 3D). Nuclear YAP/TAZ expression was restricted to basal/ME cells in terminal ductal-lobular units (TDLUs), while luminal cells exhibited diffuse cytoplasmic localization of YAP and TAZ in lobules and only occasional nuclear staining in larger-diameter ducts (Figure 3F). Co-immunofluorescence staining for TAZ and KRT14 confirmed that TAZ was frequently expressed in the nuclei of basal cells in a punctate pattern (Figure 3E).

We next asked whether TAZ expression was correlated with target gene activation. Two canonical YAP/TAZ targets, *CTGF* and *ANKRD1*, were more highly expressed in basal cells, although for *CTGF* the change did not reach statistical significance (Figure 3G). To more broadly analyze YAP/TAZ-dependent transcription in basal and luminal cells, we used publicly available gene expression data to generate a consensus signature of YAP/TAZ transcriptional targets (Cordenonsi et al., 2011; Zhang et al., 2009; Zhang et al., 2008), and tested the enrichment of the YAP/TAZ signature in previously published gene expression profiles from the various mammary epithelial subpopulations (Lim et al., 2010; Raouf et al., 2008; Shehata et al., 2012). As expected, the YAP/TAZ signature was significantly enriched in the basal/MaSC subpopulation of both human and mouse mammary epithelia, while luminal cells lacked enrichment of the TAZ signature (Figure 3H). Similar results were obtained when we queried multiple, independent gene expression datasets for enrichment of YAP/TAZ targets in the mammary epithelial subpopulations, testifying to the robustness of the association between YAP/TAZ signaling and the basal/MaSC differentiation state (Figure S2C-E). Thus, we conclude that TAZ is transcriptionally active only in basal cells in human and mouse mammary tissues, exhibiting a spatial distribution consistent with a role in regulation of lineage commitment.

TAZ is necessary for maintenance of the basal/ME lineage *in vivo*

The restricted expression pattern of TAZ in mouse and human tissues prompted us to ask whether TAZ loss also affects lineage commitment *in vivo*. We therefore examined the mammary glands of TAZ mutant mice (*Wwtr1$^{lacZ/lacZ}$*) mice, in which exon 2 of *Taz/Wwtr1* was replaced with a lacZ-stop reporter cassette (Tian et al., 2007). As previously reported, *Wwtr1$^{lacZ/lacZ}$* mice were viable but were born at sub-Mendelian ratios, with only ~20% of the expected numbers born from heterozygous crosses, and also exhibited a high perinatal mortality rate (Figure S3A-B). TAZ mRNA was not detectable in the mammary glands of *Wwtr1^{lacZ}* animals by qPCR (not shown).

We performed whole-mount staining of mammary glands of nulliparous *Wwrt1$^{+/+}$*, *Wwtr1$^{+/lacZ}$* mice, and *Wwtr1$^{lacZ/lacZ}$* mice at various developmental stages including pubescent (5 and 8 weeks old), as well as post-pubertal virgin (16 weeks old), to evaluate

gross epithelial structure. In pubescent 5 and 8 week old mice, when the primordial mammary tree is undergoing branching morphogenesis and invading into the fat pad, we did not observe any differences between wild-type, heterozygous, or homozygous $Wwtr1^{lacZ}$ glands (Figures S3C-E). Heterozygous and homozygous eight-week-old mice had a similar number of terminal end buds, which invaded into the fat pad at a similar rate and gave rise to a similar number of primary branches. However, post-pubertal 16 week-old $Wwtr1^{+/lacZ}$ and $Wwtr1^{lacZ/lacZ}$ mice exhibited a significant reduction in the number and complexity of tertiary side branching, with homozygotes displaying a more serious defect (Figures 4A and 4B). Histological analysis also revealed an overall reduction in the cross-sectional area of the fat pad occupied by epithelium in $Wwtr1^{+/lacZ}$ and $Wwtr1^{lacZ/lacZ}$ mammary glands, consistent with a general decrease in mammary gland cellularity and branching complexity (Figure 4C).

Existing ducts and lobules in 16-week old $Wwtr1^{lacZ}$ mammary glands were morphologically normal and contained a single layer of luminal and basal/ME cells (Figure S3F). However, we observed that the density of nuclei in the basal/ME layer of $Wwtr1^{lacZ/lacZ}$ ducts was noticeably sparser than in wild-type epithelia. To directly visualize luminal and basal cells *in situ*, paraffin-embedded cross-sections of $Wwtr1^{lacZ}$ mammary glands were co-stained with antibodies against EpCAM and alpha-smooth muscle actin (SMA) and analyzed by immunofluorescence microscopy (Figures 4D-E). Wild-type, heterozygous and homozygous $Wwtr1^{lacZ}$ ducts all displayed restricted expression of EpCAM and SMA to the luminal and basal layers, respectively. However, the proportion of SMA+ nuclei was dramatically reduced in $Wwtr1$-deficient epithelia, indicating a reduced number of myoepithelial cells (Figure 4E). A modest decease in the number of basal/ME cells was also observed in heterozygous animals. To further confirm this observation, we analyzed freshly dissociated MECs from 16-week-old mice of all three genotypes using flow cytometry for additional lineage-specific markers. Analysis of $Wwtr1^{+/lacZ}$ and $Wwtr1^{lacZ/lacZ}$ MECs revealed an abnormal balance of Lin^{-}CD49f^{low}CD24^{high} luminal cells vs. Lin^{-}CD49f^{high}/CD24+ basal/ME cells, compared with age-matched wild-type mice (Figures 4F and 4G). While wild-type epithelia contained roughly equal proportions of basal and luminal cells, TAZ-deficient mammary glands harbored between two and five luminal cells per basal cell, depending on the individual. As with the morphologic defects, there was no difference in the ratio of basal and luminal cells during puberty (Figures S3G-H), again suggesting TAZ is likely dispensable in the mammary gland at earlier developmental stages.

Cells in the mammary gland occasionally proliferate, which maintains the pool of epithelial cells during homeostasis (Clarke, 2003). Given the pro-proliferative effects of TAZ in basal MCF10A cells, we asked whether branching defects and altered subpopulation sizes in $Wwtr1^{lacZ}$ mammary glands might simply explained by a proliferative imbalance between the two lineages. However, surprisingly, after accounting for the reduced cellularity of $Wwtr1^{lacZ}$ epithelia, there was no statistically significant difference in either the total number of Ki67-positive proliferating cells vs. wild-type glands, or in the number of Ki67+ basal vs. luminal cells (Figure 4H). Therefore, it is unlikely that the observed lineage imbalance in $Wwtr1^{lacZ}$ mice is due to a relative reduction of proliferative capacity in basal cells or an increased rate of proliferation in luminal cells. We therefore wondered whether a

loss or exhaustion of basally-oriented progenitor cells might instead underlie the phenotype of *Wwtr1*-deficient mice. To evaluate progenitor activity, we subjected MECs isolated from 16-week old mice to an *in vitro* colony-forming assay. *Wwtr1+/lacZ and Wwtr1lacZ/lacZ* MECs formed fewer KRT14+ colonies than wild-type cells, although in the case of the heterozygotes, the difference did not reach statistical significance (Figure 4I). Collectively, these data suggest that either *Wwtr1lacZ* mice lack sufficient basal progenitor cells to maintain the lineage, or alternatively, that these cells sometimes produce luminal progeny.

SWI/SNF chromatin-remodeling complexes mediate the function of TAZ

We next sought to identify the mechanism by which TAZ influences cell fate and progenitor activity in MECs. TAZ lacks a DNA-binding domain, but is capable of activating gene expression by binding to other transcription factors such as TEADs and SMADs via conserved protein-protein interaction domains (Sudol et al., 1995, Chen and Sudol, 1995). However, very little is known about the mechanism by which TAZ binding leads to transcriptional activation. To identify binding partners of TAZ that may participate in regulation of MEC lineage commitment, we performed co-immunoprecipitation of FLAG-tagged TAZ followed by mass spectrometry (IP/MS). Using this approach, we identified 102 high-confidence binding partners, including many of the known YAP/TAZ interactants such as angiomotin (AMOT), 14-3-3 proteins, and many components of the apical junction/ polarity complex (Table S2). Of particular interest among the set of interacting proteins identified by IP/MS were several components of the SWI/SNF chromatin-remodeling complex, including the core subunits BAF155, BAF170, SNF5, and the catalytic ATPase component, which can include either BRG1 or BRM, but not both (Figure 5A). SWI/SNF is a set of evolutionarily conserved, multi-protein complexes capable of destabilizing the interaction between DNA and nucleosomes in an ATP-dependent manner, leading to nucleosome sliding or ejection and modification of higher-order chromatin structure (Müller and Leutz, 2001; Wang et al., 1996). By affecting the state of chromatin at promoter regions, SWI/SNF complexes can affect transcription factor accessibility and either repress or activate transcription.

We confirmed the presence of a protein-protein interaction between endogenous TAZ and the SWI/SNF catalytic subunit BRG1 in MCF10A cells by co-IP (Figure 5B). Upon inspection of the peptide sequences of various SWI/SNF subunits, we found that multiple SWI/SNF components contain one or more L/P-P-X-Y motifs, a binding site for the WW domain of YAP and TAZ (Figure S4). Indeed, deletion of the WW domain of TAZ abolished the interaction with BRG1 or BRM, suggesting a direct and specific interaction between the WW domain of TAZ and at least one of the PPXY-containing SWI/SNF subunits (Figure 5C and 5D). Interestingly, the PPXY motifs were conserved in vertebrates but generally not in lower eukaryotes, suggesting that the TAZ-SWI/SNF interaction may be a relatively recent evolutionary innovation (Figure S4).

We hypothesized that SWI/SNF complexes might mediate the function of TAZ to regulate transcription and lineage commitment in MECs. As the nucleosome-remodeling function of SWI/SNF complexes requires the presence of the ATPase subunit (Phelan et al., 1999), we focused on modulating BRG1 and BRM levels in MECs. We used lentivirus to stably knock

down either BRG1 or BRM in MCF10F cells and asked whether BRG1 depletion could recapitulate the features of TAZ loss (Figure 5E).

Depletion of BRG1 did not affect expression of *CTGF* or *ANKRD1*, suggesting that BRG1 is dispensable for transcription of TAZ target genes. On the other hand, BRM knockdown led to a substantial decrease in *CTGF* and *ANKRD1* mRNA levels (Figure 5F), despite compensatory upregulation of BRG1 (Figure 5E). Furthermore, stable TAZ overexpression and subsequent BRM/BRG1 knockdown using lentivirus demonstrated that BRM, but not BRG1 depletion could reverse the TAZ-mediated expansion of basal CD44^{high}/EpCAM^{low} cells in the MCF10F cell line; upon BRM knockdown, the relative sizes of the luminal and basal subpopulations of MCF10F-TAZ cells reverted to those of the lacZ control cell line (Figure 5G and 5H). Similarly BRM, but not BRG1 knockdown could rescue the activation of basal-specific genes *CD44* and *VIM* by TAZ in MCF10F cells (Figure 5I). Finally, analysis of the gene expression data from Lim et al. (2010) revealed that the pattern of BRM mRNA expression in mammary epithelial subsets mirrored the expression of TAZ and its target genes, being more highly expressed in the basal/MaSC subpopulation than in luminal cells, which is consistent with a functional interaction between TAZ and BRM *in vivo* (Figure 5J). On the other hand, BRG1 expression showed no statistical differences between epithelial subsets, consistent with its inability to affect transcription of TAZ targets.

To determine whether TAZ could directly recruit BRG1/BRM to target genes, we performed chromatin immunoprecipitation (ChIP) in MCF10A cells. We observed enrichment of BRM, but not BRG1 at the *CTGF* promoter, a *bona fide* direct target of TAZ/TEAD (Figure 5K). Furthermore, while overexpression of wild-type TAZ in MCF10A increased BRM enrichment two-fold at the *CTGF* gene, the WW mutant lacked this capacity. Instead, it repressed enrichment of BRM below background levels, suggesting it could out-compete endogenous TAZ for *CTGF* binding sites.

Taken together, these data demonstrate that BRM recruited by TAZ to regulate target gene expression, and that TAZ requires BRM to repress luminal differentiation in mammary epithelial cells. Although TAZ retains the ability to bind to BRG1 in MCF10A cells (Figure 5B), we were not able to identify a functional consequence of this interaction in the context of MEC differentiation.

TAZ is amplified in basal-like breast cancer

Lastly, we asked whether TAZ might also influence breast tumor phenotype. Although the majority of breast cancers originate from the transformation of luminal cells, the resulting tumors can exhibit features of either luminal or basal differentiation at the histological and molecular level (Keller et al., 2012; Prat and Perou, 2011). Interestingly, analysis of data from The Cancer Genome Atlas (TCGA, Koboldt et al., 2012) revealed that 44% of basal-like breast tumors exhibited some degree of *TAZ* copy number amplification, compared to only 10 and 20% of luminal A and luminal B tumors, respectively (Figure 6A). Concordantly, TAZ mRNA expression was much higher in basal-like tumors than in luminal tumors from the TCGA dataset (Figure 6B). Furthermore, TAZ expression was negatively correlated with the protein level of key luminal biomarkers such as *GATA3*, estrogen receptor, and androgen receptor (False Discovery Rate [FDR[= 0%), and positively

associated with protein levels of basal biomarkers (FDR = 0%), as measured by reverse-phase protein arrays (Figure 6C). TAZ protein levels were also much higher in basal-like breast cancer cell lines than in luminal-like cell lines (Figure 6D). Importantly, high TAZ expression predicted poor survival in patients with basal-like tumors, but not in other molecular subtypes, in accordance with the known oncogenic role of TAZ (Figure 6E). Collectively and in light of the role of TAZ in lineage commitment, these data suggest that high expression of TAZ may bias breast tumors toward a basal-like phenotype and promote disease progression.

Discussion

Our initial goal was to identify novel regulators of mammary epithelial cell fate in a manner that was both biologically relevant and human-oriented. We employed an innovative screening approach designed to exploit a key functional distinction between basal and luminal epithelial cells – namely, their ability to grow as adherent colonies on a plastic substrate. We posit that a similar approach in other systems can complement the use of murine genetic screens in the search for regulators of human development, as mouse models do not always faithfully recapitulate human biology. However, the use of primary cells derived from human tissue is critical, as it is well known that many cells, including MECs do not maintain their identity after extended culture *in vitro*.

Our findings broadly imply that cellular differentiation states may be dynamically regulated in normal cells and tissues via the activation or inactivation of specific transcriptional factors. Lineage-tracing studies have definitively demonstrated the restricted nature of the luminal lineage of the mammary gland during homeostasis (Van Keymeulen et al., 2011; Van Amerongen et al., 2012; Rios et al., 2014). However, it is clear that luminal cell fate decisions are not permanent, and can be reversed following *in vitro* culture or tumorigenesis. The most striking finding of our study is the demonstration that modulation of a single factor, TAZ, is capable on its own of dictating the differentiation state of mammary epithelial cells – allowing luminal cells to adopt basal/ME features when overexpressed, or inducing basal/ME cells to acquire luminal characteristics when depleted. In other words, TAZ acts as molecular switch regulating luminal and basal phenotypes, and toggling of the switch is sufficient to alter differentiation state.

Our results also imply that Hippo signaling plays an important role in regulating lineage dynamics in the mammary gland through modulation of YAP/TAZ subcellular localization. Hippo signaling appears to be active only in luminal cells, restricting TAZ to the cytoplasm, while in basal cells YAP and TAZ can freely influence transcription of target genes. The upstream regulation of Hippo signaling is an area of intensive research, but it is clear that cell-cell junctions and polarity signals are strong negative regulators of YAP/TAZ and that apical junction-associated signaling molecules such as angiomotin (*AMOT*) regulate the Hippo core kinases (Chen et al., 2010; Grusche et al., 2010). In the mammary gland, only luminal cells are polarized and exhibit extensive cell-cell contacts, suggesting a scenario where TAZ is continuously kept in check by Hippo signaling in cells that maintain luminal features, *i.e.* those cells that express adherens/tight junction molecules and maintain apicobasal polarity. Intriguingly, these very same features are invariably lost in contexts

where luminal-to-basal plasticity is seen, for example in cancer and *ex vivo* culture. We propose that such a mechanism might underlie the lineage-restriction of luminal cells observed in normal homeostasis, and when perturbed may result in lineage infidelity.

The lineage imbalances that result when TAZ is lost *in vivo* during development may also reflect an essential role of TAZ in maintaining the lineage fidelity of basal cells. However, given the current controversy regarding the existence of bipotent stem cells in the mammary gland within the basal layer, this finding must be cautiously interpreted. On the one hand, TAZ loss in unipotent basal progenitors may promote their trans-diffferentiation toward a luminal cell fate. Alternatively, TAZ loss in bipotent MaSCs (assuming their presence in adult tissues) may bias these cells to differentiate along the luminal lineage at an inappropriately high rate. In both scenarios, the consequence would be a loss of basal progenitors and an expansion of the luminal cell compartment similar to that seen in TAZ-null mice. As the cellular hierarchy of the mammary epithelium is further resolved, it should be possible to define which of these alternatives reflects the precise role of TAZ in MEC lineage commitment.

We also demonstrated a tissue-level requirement for TAZ during development, being required for epithelial side branching in adult virgin glands. As basal/ME cells are essential for initiating side branching (Ewald et al., 2008; Gudjonsson et al., 2005), this defect likely reflects the decreased proportion of basal cells in TAZ-null glands. Interestingly, TAZ was seemingly dispensable for ductal invasion throughout the course of pubertal development. This result suggests a functional or molecular distinction between progenitor cells that are active during puberty versus in the adult virgin epithelium. Such a notion is supported by a recent lineage tracing study demonstrating that Wnt-responsive progenitor cells contribute variably to the luminal and basal lineages depending on the developmental stage when the cells are genetically labeled (Van Amerongen et al. 2012). Specifically, prepubescent and pubescent Wnt-responsive cells contribute to ductal invasion during puberty and are unipotent, while individual Wnt-response cells in adult virgin glands drive alveologenesis and may have the potential to generate both luminal and basal cells during pregnancy and lactation. Given that TAZ mediates Wnt signaling (Azzolin et al. 2012, Rosenbluh et al. 2012), the functional differences between Wnt-responsive progenitors may underlie the stage-specific requirement for TAZ in mammary gland development. However, additional studies will be needed to more completely and precisely define the role of TAZ in mammary gland development, including an investigation of the role of TAZ during pregnancy and lactation.

A significant finding of our study is the notion that TAZ depends on chromatin-remodeling factors to effect changes in differentiation state. We showed that the SWI/SNF complex directly interacts with TAZ and is essential in mediating TAZ function. Our results expand upon recent work in *Drosophila* demonstrating that Brahma (Brm) interacts with Yki/Sd (the fly homologs of YAP/TAZ and TEADs, respectively) and regulates expression of Yki/Sd targets in the fly midgut (Jin et al., 2013; Oh et al., 2013). Our results also imply a functional distinction between BRG1 and BRM, in that only BRM could be recruited by TAZ to regulate target genes. Both BRG1 and BRM retain the ability to bind to TAZ through their PPXY motifs; therefore, we speculate that the lack of redundancy between

BRM and BRG1 may result from binding to distinct sets of cofactors or other transcription factors that provide specificity for particular promoter sequences. It is worth nothing that, while BRG1 does not seem to be important for TAZ-mediated transcription in MECs, we cannot rule out the possibility that it might regulate TAZ target genes in other cell types.

Finally, the finding that TAZ is associated with basal-like breast cancer is relevant to the understanding of breast cancer heterogeneity, since basal and luminal molecular subtypes of breast cancer share many features with their normal counterparts (Prat et al., 2013). The Hippo pathway is dysregulated or inactivated in many human cancers, including breast cancer (Pan, 2010); TAZ itself promotes proliferation and migration of breast cancer cells, and has recently been linked to the cancer stem cell (CSC) phenotype and EMT in breast cancer cell lines (Cordenonsi et al., 2011). We found that TAZ is particularly highly expressed in basal and/or triple-negative breast cancers, reflecting its expression in normal epithelia (Figure 6), and our results suggest that the high expression of TAZ in basal-like tumors likely results from copy-number amplification. The finding that TAZ is amplified in basal tumors and is also a prognostic marker strongly implies that TAZ may act as an oncogenic driver specifically in basal-like tumors. The previously unrecognized role of TAZ in lineage commitment, however, prompts the more profound question of whether genetic amplification of *TAZ* is actually deterministic of the basal-like tumor phenotype. This notion, if true, would have sweeping implications for our understanding of the histogenesis of breast cancer subtypes.

Experimental Procedures

Cell Lines and Tissue Culture

Disease-free reduction mammoplasty specimens were obtained from Tufts Medical Center in compliance with institutional and federal guidelines. Primary human MECs were isolated from fresh tissues as described previously (see Keller et al., 2012 and Extended Experimental Procedures). For all assays involving primary human MECs, cells were cultured in mammary epithelial growth medium (MEGM, Lonza). MCF10A and MCF10F cells were obtained from American Type Culture Collection (ATCC) and cultured according to ATCC's recommended methods. For additional details see Extended Experimental Procedures.

Isolation of HMEC Subpopulations

For the initial TF screen, EpCAM+ luminal cells were FACS-purified using an Influx Cell Sorter (BD) after staining primary MECs with APC-conjugated EpCAM antibody (BD #347200, 10 μl per million cells sorted). For analysis of Hippo signaling and TAZ expression in basal and luminal MEC subpopulations, primary MECs were sorted using immunomagnetic beads conjugated to anti-CD10 antibody (clone SS2/36, Santa Cruz) or anti-EpCAM antibody (clone VU-ID9, AbD Serotec), as described previously (Keller et al., 2012). Briefly, antibodies were first conjugated to CELLection pan-mouse IgG immunomagnetic beads (Life Technologies), followed by sequential incubation with primary HMEC, as depicted in Figure 3A, to generate three sorted fractions. Bound cells were released from the beads following incubation with DNase (50 ug/ml, Roche).

Lentivirus Production and Lentiviral DNA Constructs

Packaging of replication-defective lentivirus for infection has been previously described (Keller et al. 2012). Protocols for lentivirus production and generation of stable cell lines are detailed in Extended Experimental Procedures. Wild-type TAZ-FLAG and mutant TAZ-FLAG constructs were obtained from Addgene (deposited by Jeff Wrana) and were cloned into the pLenti 6.2/V5 DEST vector using the Gateway system (Life Technologies). shRNA constructs were obtained from Sigma's MISSION RNAi library. A complete list of all expression and shRNA vectors used to generate stable cell lines can be found in Extended Experimental Procedures.

2D and 3D Colony Forming Assays

For adherent colony forming assays involving primary human and mouse MECs, 40,000 cells were seeded into 6-well plates, propagated for 10 days, fixed in 10% neutral buffered formalin, and stained with either 0.1% crystal violet or KRT14 and KRT18 antibodies (see Immunostaining) to visualize and quantify colonies. For mammosphere assays, 10,000 primary MECs or 5,000 MCF10A cells were seeded in 6-well ultra-low attachment tissue culture plates (Corning) and propagated for five days. The entire 2 ml culture was then diluted in a 3:2 mixture of Isoton II (Beckman Coulter) and glycerol, and analyzed using a Multisizer 3 cytometer (Beckman Coulter). All particles meeting the 30-μm-diameter cutoff were considered to be mammospheres. For 3D collagen assays, 10,000 primary HMECs or 1,000 MCF10A/MCF10F cells were overlaid on 4-well chamber slides (BD Falcon) coated with 1 mg/ml type I collagen (Millipore, pH 7.0) and supplemented with 2% Matrigel (BD Biosciences), solubilized in the growth medium. Cultures were allowed to propagate for 14 days, followed by microscopic analysis of the colony morphologies.

Quantitative RT-PCR and Nanostring nCounter Analysis

For all qPCR experiments, total RNA was extracted using the RNeasy Mini Kit (Qiagen). cDNA was prepared from 1 ug of total RNA with the iScript kit (BioRad) according to the manufacturer's instructions. qPCR was performed using SYBR Green Supermix (BioRad) on a CFX96 Real-time Thermal Cycler (BioRad). Threshold cycle numbers were converted to relative gene expression values using the $2^{-\Delta Ct}$ method. Primer sequences, as well as additional information regarding nCounter gene expression analysis, are available in Extended Experimental Procedures.

Flow Cytometry

For analysis of adherent cell lines, cells were harvested by trypsinization, resuspended at 10^6/ml in PBS with 1% calf serum, and stained for 15 minutes at room temperature with the appropriate antibodies at the appropriate dilutions. For flow cytometry of mouse MECs, the bilateral 3rd, 4th, and 5th mammary glands were harvested, minced with scissors, digested in collagenase, hyaluronidase, and trypsin to yield a single cell suspension, and stained as above. Mouse MECs were additionally stained with PE-conjugated anti-TER119, anti-CD31, and anti-CD45 antibodies ("Lin" stain), to allow for gating of Lin^{+} cells. All analytic flow cytometry was carried out on a FACScalibur (BD), while sorting of EpCAM/CD44 subpopulations of MCF10F cells was performed on a MoFlo cell sorter (Beckman Coulter).

Flow cytometry data was analyzed using FlowJo software. For a complete list of specific antibodies and dilutions used in flow cytometry, see Extended Experimental Procedures.

Animals

All experiments involving animal subjects were carried out with the approval of the Tufts University IACUC. 129S-*Wwtr1^{tm1Benj}* mice were obtained from Jackson Laboratories (Stock Number 011120, the mutant allele is referred to as *Wwtr1^{lacZ}* in the text). Mice were maintained on the 129S background for all studies by heterozygous crosses. For whole mount analyses of mammary glands, the 4th mammary gland was dissected and fixed overnight in 10% neutral buffered formalin, followed by 1-3 days of staining in 0.2% carmine aluminum dye (Sigma). Glands were subsequently dehydrated in graded ethanols, cleared by 1-3 days incubation in xylenes, and transferred to glycerol for long-term storage.

Supplementary Material

Refer to Web version on PubMed Central for supplementary material.

Acknowledgments

References

Azzolin L, Zanconato F, Bresolin S, Forcato M, Basso G, Bicciato S, Cordenonsi M, Piccolo S. Role of TAZ as mediator of wnt signaling. Cell. 2012; 151:1443–1456. [PubMed: 23245942]

Chaffer CL, Brueckmann I, Scheel C, Kaestli AJ, Wiggins PA, Rodrigues LO, Brooks M, Reinhardt F, Suc Y, Polyak K, et al. Normal and neoplastic nonstem cells can spontaneously convert to a stem-like state. Proc Natl Acad Sci U S A. 2011; 108:7950–7955. [PubMed: 21498687]

Chen C, Gajewski KM, Hamaratoglu F, Bossuyt W, Sansores-Garcia L, Tao C, Halder G. The apical-basal cell polarity determinant Crumbs regulates Hippo signaling in Drosophila. Proc Natl Acad Sci U S A. 2010; 107:15810–15815. [PubMed: 20798049]

Chen HI, Sudol M. The WW domain of Yes-associated protein binds a proline-rich ligand that differs from the consensus established for Src homology 3-binding modules. Proc Natl Acad Sci U S A. 1995; 92:7819–7823. [PubMed: 7644498]

Clarke RB. Steroid receptors and proliferation in the human breast. Steroids. 2003; 68:789–794. [PubMed: 14667969]

Cordenonsi M, Zanconato F, Azzolin L, Forcato M, Rosato A, Frasson C, Inui M, Montagner M, Parenti AR, Poletti A, et al. The hippo transducer TAZ confers cancer stem cell-related traits on breast cancer cells. Cell. 2011; 147:759–772. [PubMed: 22078877]

Ewald AJ, Brenot A, Duong M, Chan BS, Werb Z. Collective Epithelial Migration and Cell Rearrangements Drive Mammary Branching Morphogenesis. Developmental Cell. 2008; 14:570–581. [PubMed: 18410732]

Galliot B, Ghila L. Cell plasticity in homeostasis and regeneration. Mol Reprod Dev. 2010; 77:837–855. [PubMed: 20602493]

Grusche FA, Richardson HE, Harvey KF. Upstream regulation of the Hippo size control pathway. Current Biology. 2010; 20:574–582.

Gudjonsson T, Adriance MC, Sternlicht MD, Petersen OW, Bissell MJ. Myoepithelial cells: their origin and function in breast morphogenesis and neoplasia. J Mammary Gland Biol Neoplasia. 2005; 10:261–272. [PubMed: 16807805]

Jin Y, Xu J, Yin M, Lu Y, Hu L, Li P, Zhang P, Yuan Z, Ho MS, Zhao Y, Zhang L. Brahma is essential for Drosophila intestinal stem cell proliferation and regulated by hippo signaling. eLife. 2013; 2013

Keller PJ, Arendt LM, Skibinski A, Logvinenko T, Klebba I, Dong S, Smith AE, Prat A, Perou CM, Gilmore H, et al. Defining the cellular precursors to human breast cancer. Proc Natl Acad Sci U S A. 2012; 109:2772–2777. [PubMed: 21940501]

Koboldt DC, Fulton RS, McLellan MD, Schmidt H, Kalicki-Veizer J, McMichael JF, Fulton LL, Dooling DJ, Ding L, Mardis ER, et al. Comprehensive molecular portraits of human breast tumours. Nature. 2012; 490:61–70. [PubMed: 23000897]

Kordon EC, Smith GH. An entire functional mammary gland may comprise the progeny from a single cell. Development. 1998; 125:1921–1930. [PubMed: 9550724]

Lei Q, Zhang H, Zhao B, Zha Z, Bai F, Pei X, Zhao S, Xiong Y, Guan K. TAZ promotes cell proliferation and epithelial-mesenchymal transition and is inhibited by the hippo pathway. Mol Cell Biol. 2008; 28:2426–2436. [PubMed: 18227151]

Lim E, Wu D, Pal B, Bouras T, Asselin-Labat M, Vaillant F, Yagita H, Lindeman GJ, Smyth GK, Visvader JE. Transcriptome analyses of mouse and human mammary cell subpopulations reveal multiple conserved genes and pathways. Breast Cancer Research. 2010; 12

Molyneux G, Geyer FC, Magnay F, McCarthy A, Kendrick H, Natrajan R, MacKay A, Grigoriadis A, Tutt A, Ashworth A, Reis-Filho JS, Smalley MJ. BRCA1 basal-like breast cancers originate from luminal epithelial progenitors and not from basal stem cells. Cell Stem Cell. 2010; 7:403–417. [PubMed: 20804975]

Müller C, Leutz A. Chromatin remodeling in development and differentiation. Current Opinion in Genetics and Development. 2001; 11:167–174. [PubMed: 11250140]

Oh H, Slattery M, Ma L, Crofts A, White KP, Mann RS, Irvine KD. Genome-wide Association of Yorkie with Chromatin and Chromatin-Remodeling Complexes. Cell Reports. 2013; 3:309–318. [PubMed: 23395637]

Pan D. The hippo signaling pathway in development and cancer. Developmental Cell. 2010; 19:491–505. [PubMed: 20951342]

Péchoux C, Gudjonsson T, Rønnov-Jessen L, Bissell MJ, Petersen OW. Human mammary luminal epithelial cells contain progenitors to myoepithelial cells. Dev Biol. 1999; 206:88–99. [PubMed: 9918697]

Phelan ML, Sif S, Narlikar GJ, Kingston RE. Reconstitution of a core chromatin remodeling complex from SWI/SNF subunits. Mol Cell. 1999; 3:247–253. [PubMed: 10078207]

Prat A, Karginova O, Parker JS, Fan C, He X, Bixby L, Harrell JC, Roman E, Adamo B, Troester M, Perou CM. Characterization of cell lines derived from breast cancers and normal mammary tissues for the study of the intrinsic molecular subtypes. Breast Cancer Res Treat. 2013; 142:237–255. [PubMed: 24162158]

Prat A, Perou CM. Deconstructing the molecular portraits of breast cancer. Molecular Oncology. 2011; 5:5–23. [PubMed: 21147047]

Proia TA, Keller PJ, Gupta PB, Klebba I, Jones AD, Sedic M, Gilmore H, Tung N, Naber SP, Schnitt S, Lander ES, Kuperwasser C. Genetic predisposition directs breast cancer phenotype by dictating progenitor cell fate. Cell Stem Cell. 2011; 8:149–163. [PubMed: 21295272]

Raouf A, Zhao Y, To K, Stingl J, Delaney A, Barbara M, Iscove N, Jones S, McKinney S, Emerman J, et al. Transcriptome analysis of the normal human mammary cell commitment and differentiation process. Cell Stem Cell. 2008; 3:109–118. [PubMed: 18593563]

Rios AC, Fu NY, Lindeman GJ, Visvader JE. In situ identification of bipotent stem cells in the mammary gland. Nature. 2014; 506:322–327. [PubMed: 24463516]

Rompolas P, Mesa KR, Greco V. Spatial organization within a niche as a determinant of stem-cell fate. Nature. 2013; 502:513–518. [PubMed: 24097351]

Rosenbluh J, Nijhawan D, Cox AG, Li X, Neal JT, Schafer EJ, Zack TI, Wang X, Tsherniak A, Schinzel AC, et al. ß-Catenin-driven cancers require a YAP1 transcriptional complex for survival and tumorigenesis. Cell. 2012; 151:1457–1473. [PubMed: 23245941]

Santagata S, Thakkar A, Ergonul A, Wang B, Woo T, Hu R, Harrell JC, McNamara G, Schwede M, Culhane AC, et al. Taxonomy of breast cancer based on normal cell phenotype predicts outcome. J Clin Invest. 2014; 124(2):859–870. [PubMed: 24463450]

Sarrió D, Rodriguez-Pinilla SM, Hardisson D, Cano A, Moreno-Bueno G, Palacios J. Epithelial-mesenchymal transition in breast cancer relates to the basal-like phenotype. Cancer Res. 2008; 68:989–997. [PubMed: 18281472]

Shackleton M, Vaillant F, Simpson KJ, Stingl J, Smyth GK, Asselin-Labat M, Wu L, Lindeman GJ, Visvader JE. Generation of a functional mammary gland from a single stem cell. Nature. 2006; 439:84–88. [PubMed: 16397499]

Shehata M, Teschendorff A, Sharp G, Novcic N, Russell IA, Avril S, Prater M, Eirew P, Caldas C, Watson CJ. Phenotypic and functional characterisation of the luminal cell hierarchy of the mammary gland. Breast Cancer Research. 2012; 14

Soule HD, Maloney TM, Wolman SR, Peterson WD Jr, Brenz R, McGrath CM, Russo J, Pauley RJ, Jones RF, Brooks SC. Isolation and characterization of a spontaneously immortalized human breast epithelial cell line, MCF-10. Cancer Res. 1990; 50:6075–6086. [PubMed: 1975513]

Spike BT, Engle DD, Lin JC, Cheung SK, La J, Wahl GM. A mammary stem cell population identified and characterized in late embryogenesis reveals similarities to human breast cancer. Cell Stem Cell. 2012; 10:183–197. [PubMed: 22305568]

Sudol M, Bork P, Einbond A, Kastury K, Druck T, Negrini M, Huebner K, Lehman D. Characterization of the mammalian YAP (Yes-associated protein) gene and its role in defining a novel protein module, the WW domain. J Biol Chem. 1995; 270:14733–14741. [PubMed: 7782338]

Tata PR, Mou H, Pardo-Saganta A, Zhao R, Prabhu M, Law BM, Vinarsky V, Cho JL, Breton S, Sahay A, Medoff BD, Rajagopal J. Dedifferentiation of committed epithelial cells into stem cells in vivo. Nature. 2013

Tian Y, Kolb R, Hong J, Carroll J, Li D, You J, Bronson R, Yaffe MB, Zhou J, Benjamin T. TAZ promotes PC2 degradation through a SCFβ-Trcp E3 ligase complex. Mol Cell Biol. 2007; 27:6383–6395. [PubMed: 17636028]

Tsai YC, Lu Y, Nichols PW, Zlotnikov G, Jones PS, Smith HS. Contiguous patches of normal human mammary epithelium derived from a single stem cell: Implications for breast carcinogenesis. Cancer Res. 1996; 56:402–404. [PubMed: 8542598]

Van Amerongen R, Bowman AN, Nusse R. Developmental stage and time dictate the fate of Wnt/ß-catenin- responsive stem cells in the mammary gland. Cell Stem Cell. 2012; 11:387–400. [PubMed: 22863533]

Van Keymeulen A, Rocha AS, Ousset M, Beck B, Bouvencourt G, Rock J, Sharma N, Dekoninck S, Blanpain C. Distinct stem cells contribute to mammary gland development and maintenance. Nature. 2011; 479:189–193. [PubMed: 21983963]

Visvader JE. Keeping abreast of the mammary epithelial hierarchy and breast tumorigenesis. Genes and Development. 2009; 23:2563–2577. [PubMed: 19933147]

Visvader JE, Lindeman GJ. Mammary stem cells and mammopoiesis. Cancer Res. 2006; 66:9798–9801. [PubMed: 17047038]

Wang W, Côté J, Xue Y, Zhou S, Khavari PA, Biggar SR, Muchardt C, Kalpana GV, Goff SP, Yaniv M, Workman JL, Crabtree GR. Purification and biochemical heterogeneity of the mammalian SWI-SNF complex. EMBO J. 1996; 15:5370–5382. [PubMed: 8895581]

Zhang H, Liu C, Zha Z, Zhao B, Yao J, Zhao S, Xiong Y, Lei Q, Guan K. TEAD transcription factors mediate the function of TAZ in cell growth and epithelial-mesenchymal transition. J Biol Chem. 2009; 284:13355–13362. [PubMed: 19324877]

Zhang J, Smolen GA, Haber DA. Negative regulation of YAP by LATS1 underscores evolutionary conservation of the Drosophila Hippo pathway. Cancer Res. 2008; 68:2789–2794. [PubMed: 18413746]

Zhou Q, Brown J, Kanarek A, Rajagopal J, Melton DA. In vivo reprogramming of adult pancreatic exocrine cells to ß-cells. Nature. 2008; 455:627–632. [PubMed: 18754011]

Highlights

- *TAZ* controls differentiation state in mammary epithelial cell lines

- Loss of *TAZ* in mice leads to branching defects and loss of the basal/ME population

- SWI/SNF complexes bind to *TAZ* and mediate its effects on transcription

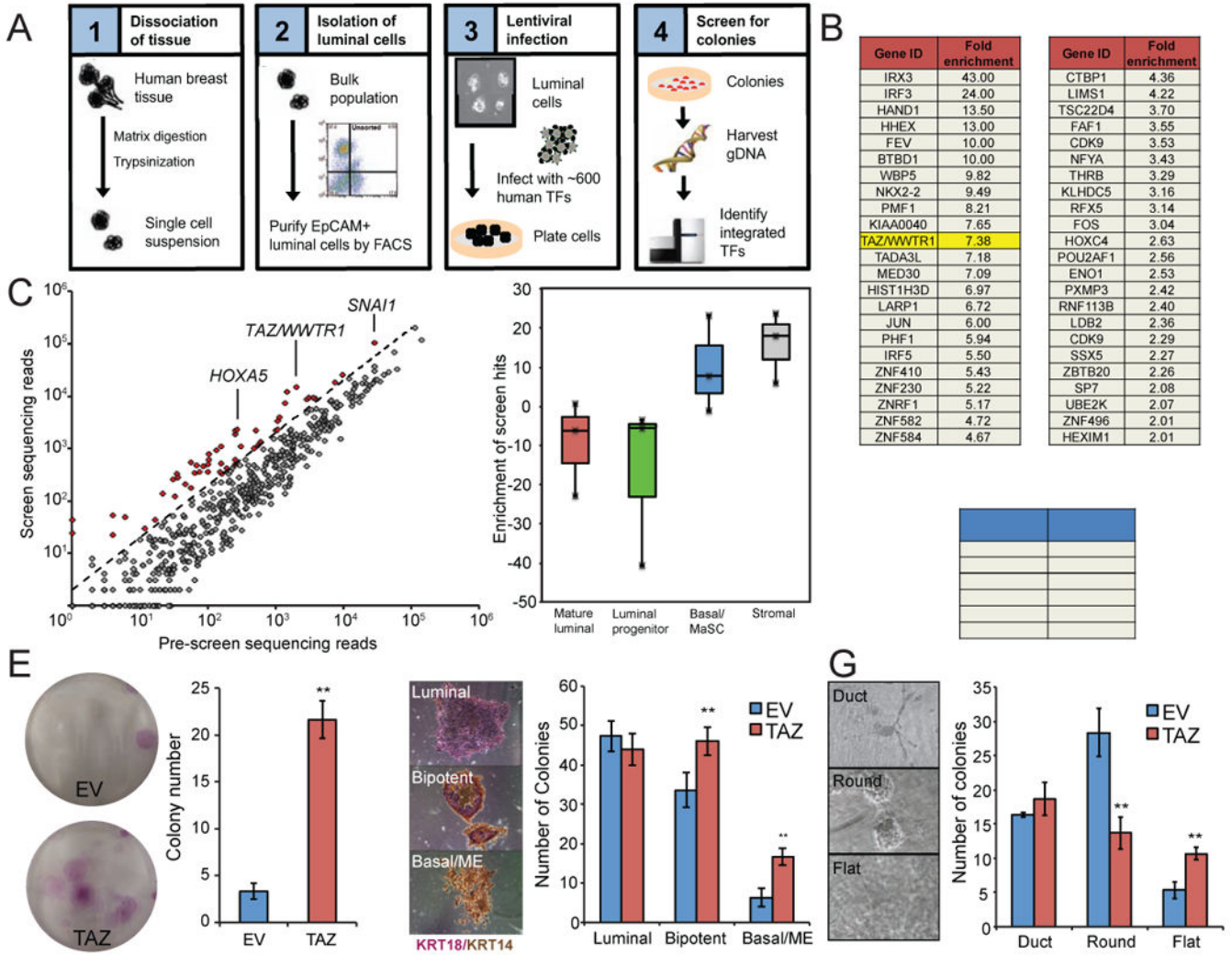- TAZ is overexpressed and amplified in basal-like breast cancer and predicts survival

A (1) Dissociation of tissue — Human breast tissue → Matrix digestion → Trypsinization → Single cell suspension. (2) Isolation of luminal cells — Bulk population → Purify EpCAM+ luminal cells by FACS. (3) Lentiviral infection — Luminal cells → Infect with ~600 human TFs → Plate cells. (4) Screen for colonies — Colonies → Harvest gDNA → Identify integrated TFs.

B

Gene ID	Fold enrichment		Gene ID	Fold enrichment
IRX3	43.00		CTBP1	4.36
IRF3	24.00		LIMS1	4.22
HAND1	13.50		TSC22D4	3.70
HHEX	13.00		FAF1	3.55
FEV	10.00		CDK9	3.53
BTBD1	10.00		NFYA	3.43
WBP5	9.82		THRB	3.29
NKX2-2	9.49		KLHDC5	3.16
PMF1	8.21		RFX5	3.14
KIAA0040	7.65		FOS	3.04
TAZ/WWTR1	7.38		HOXC4	2.63
TADA3L	7.18		POU2AF1	2.56
MED30	7.09		ENO1	2.53
HIST1H3D	6.97		PXMP3	2.42
LARP1	6.72		RNF113B	2.40
JUN	6.00		LDB2	2.36
PHF1	5.94		CDK9	2.29
IRF5	5.50		SSX5	2.27
ZNF410	5.43		ZBTB20	2.26
ZNF230	5.22		SP7	2.08
ZNRF1	5.17		UBE2K	2.07
ZNF582	4.72		ZNF496	2.01
ZNF584	4.67		HEXIM1	2.01

Figure 1. Screen for transcription factors involved in MEC lineage commitment

A, Schematic of the screening approach used to identify novel regulators of MEC fate. **B** and **C**, a list and dot plot representing the 46 identified TFs enriched greater than the two-fold cutoff (indicated by the dotted line in **C**). Enrichment scores were calculated as a fold increase over transduced but unscreened control cells ("pre-screen"). **D**, Box-and-whisker plot showing enrichment scores of the complete set of screen hits in gene expression profiles from purified mammary epithelial subsets as reported by Lim et al. (2010). **E**, MECs were isolated and sorted as in **A**, transduced with lentivirus containing TAZ cDNA, and subjected to a colony-forming assay. **F**, Unsorted MECs were transduced with TAZ cDNA and subjected to a colony-forming assay as in **E**. The colonies were co-immunostained with KRT14 (brown) and KRT18 (purple) to evaluate differentiation state (depicted in the representative images on the left). **G**, TAZ-transduced MECs were plated on 1 mg/ml collagen gels for colony formation and the colony types were quantified (classified as ductal, round/acinar, or flat as indicated in the representative images). In all panels, error bars represent the SEM. Significance values were computed by Student's t-test; a single

asterisk represent a significance level of $p < 0.05$, double asterisks indicate $p < 0.01$. All colony-forming assays were performed using cells isolated from at least three tissue donors.
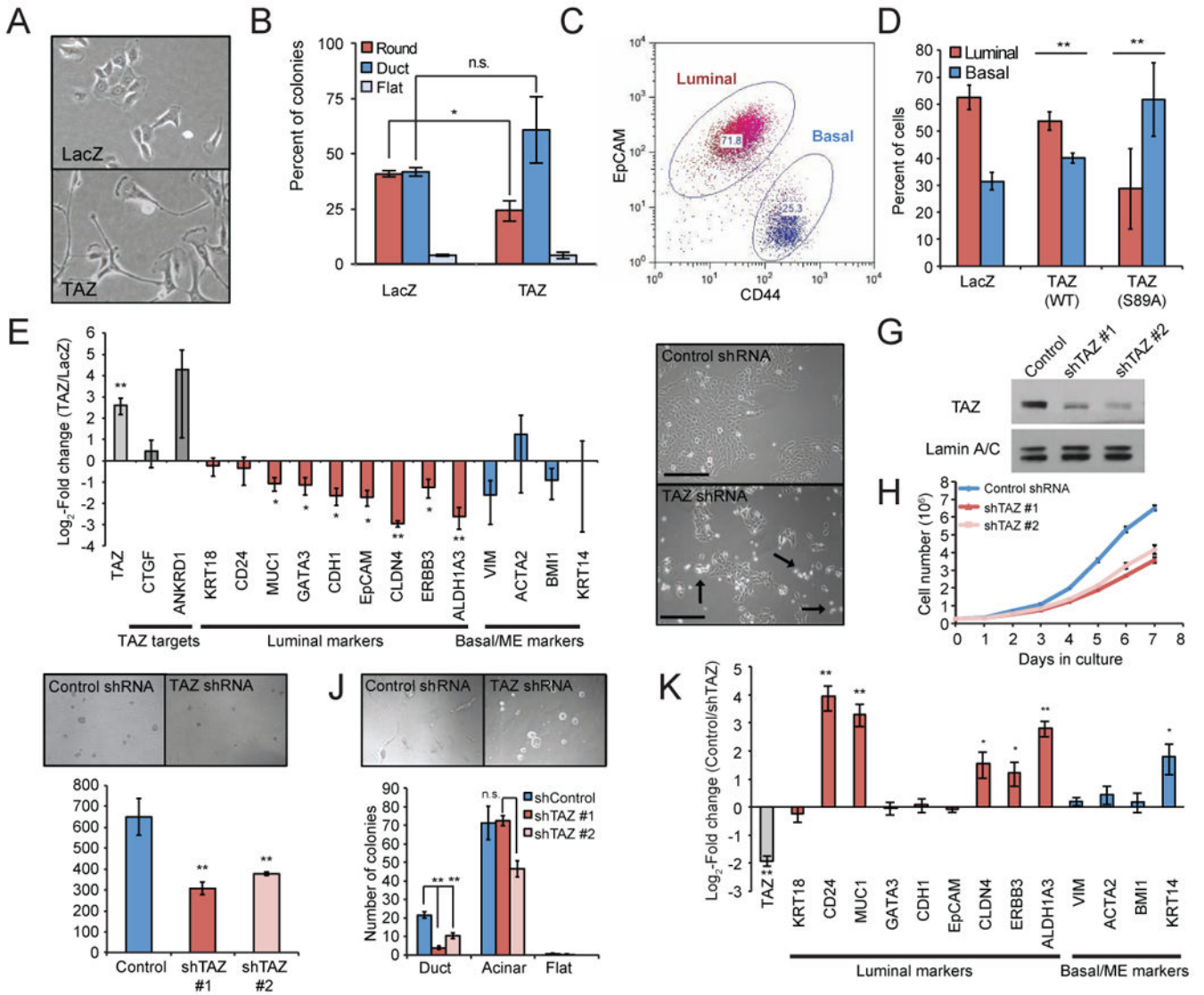
Figure 2. TAZ controls MEC differentiation state
A-F, TAZ cDNA or lacZ cDNA was expressed in MCF10F cells using lentiviral vectors (N = 3 experiments). **A**, Representative image of control MCF10F cells and MCF10F-TAZ cells. **B**, 3D colony formation in MCF10F-TAZ cells. **C**, Flow cytometry of MCF10F cells resolves EpCAM^{high}/CD44^{low} luminal-like and EpCAM$^{low/-}$/CD44^{high} basal-like subpopulations. **D**, The relative proportion of luminal and basal cells in MCF10F-TAZ was quantified by the gating strategy indicated in **C**. S89A is a Hippo-refractory mutant form of TAZ. **E**, mRNA expression of known TAZ target genes (dark grey bars), luminal markers (red bars) and basal/ME markers (blue bars) in MCF10F-TAZ cells. Values are represented as a log$_2$ fold-change over LacZ control cells. **F-K**, TAZ was depleted in MCF10A cells using shRNAs (N = 6 experiments). **F**, TAZ depletion caused many cells to become non-adherent and detach from the substrate (arrows). **G**, TAZ protein levels following transduction with shRNA constructs. **H**, Growth kinetics of MCF10A-shTAZ over 7 days. **I**, Mammospheres (> 30 μm diameter) formed by MCF10A-shTAZ cells. **J**, 3D morphogenesis

assay after MCF10A-shTAZ cells were seeded on collagen gels as in **C. K**, qRT-PCR analysis of gene expression in MCF10A cells following TAZ knockdown. Gene expression values are represented as a $\log_2$ fold change over the control cell line. In all panels, error bars represent the SEM, a single asterisk indicates $p < 0.05$ and a double asterisk represents $p < 0.01$ as determined by Student's t-test (pairwise against the control cell line). See also Figure S1.
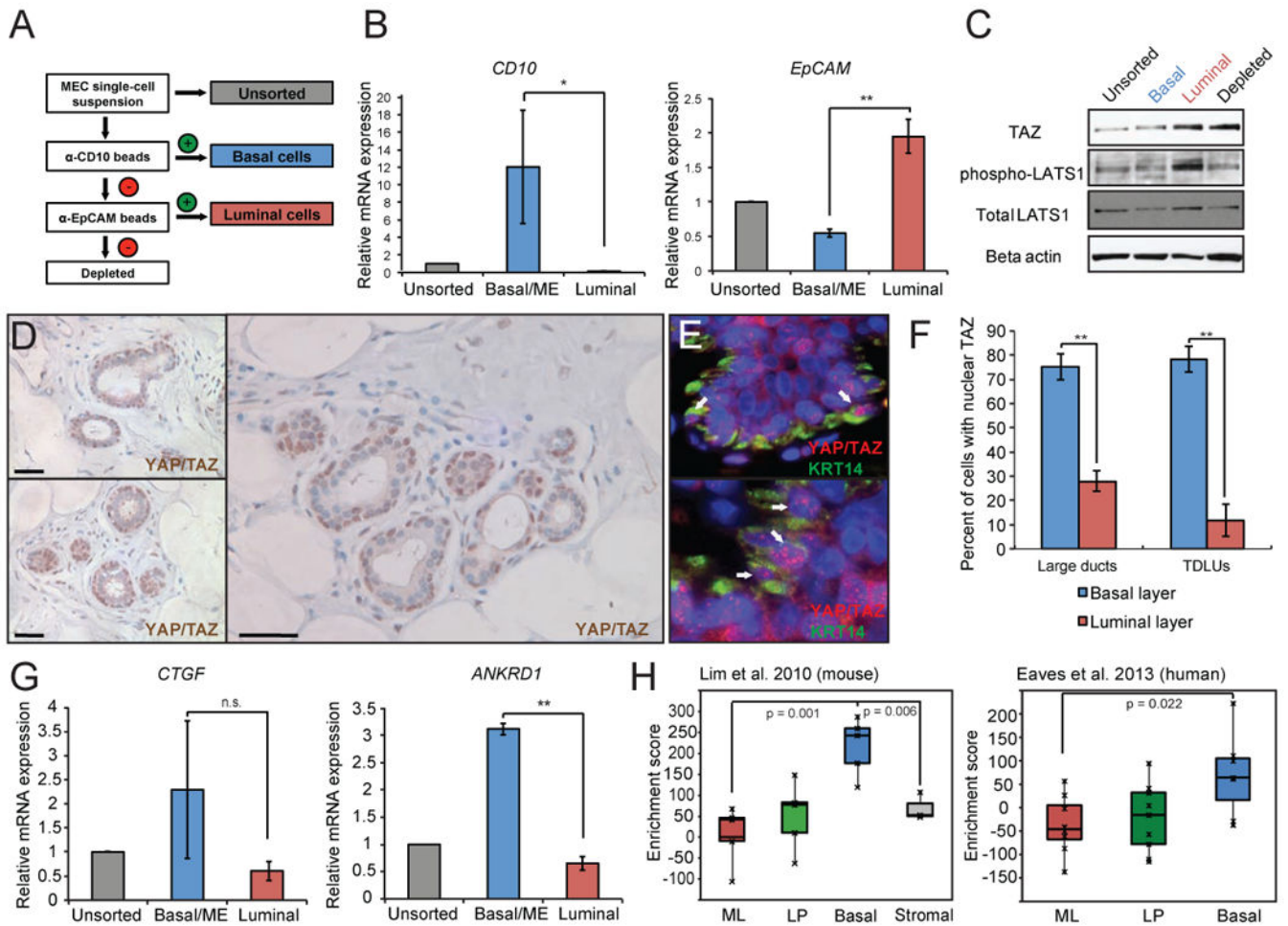
Figure 3. Lineage-specific Hippo signaling and TAZ expression in breast tissues
A, Schematic of sorting strategy used to purify luminal and basal subsets from breast reductions tissues using EpCAM and CD10 immunomagnetic beads. **B**, qRT-PCR analysis of CD10 and EpCAM expression following sorting demonstrating enrichment of the appropriate marker in the basal vs. luminal sorted cells (N = 4 tissue donors). **C**, Representative Western blot analysis of phospho-LATS1, total LATS1, and TAZ protein levels in purified luminal and basal cells. **D**, Low and high-power images of formalin fixed, paraffin-embedded human breast tissue specimens immunostained with an antibody reactive against both YAP and TAZ, demonstrating nuclear TAZ expression in basal cells. **E**, Co-immunofluorescence staining with YAP/TAZ and KRT14, a marker of basal cells, showing punctate nuclear for YAP/TAZ in K14+ cells vs. cytoplasmic staining in K14- cells (white arrows). **F**, Quantitation of the percent of cells with nuclear YAP/TAZ expression in large-diameter ducts vs. TDLUs. **G**, mRNA expression of TAZ targets *CTGF* and *ANKRD1* in sorted subpopulations. **H**, Enrichment analysis of the TAZ target gene signature in microarray datasets of purified mouse and human MEC subpopulations. In all panels, error bars represent the SEM, a single asterisk indicates *p* < 0.05 and double asterisks represents *p* < 0.01 as determined by Student's t-test. See also Figure S2.
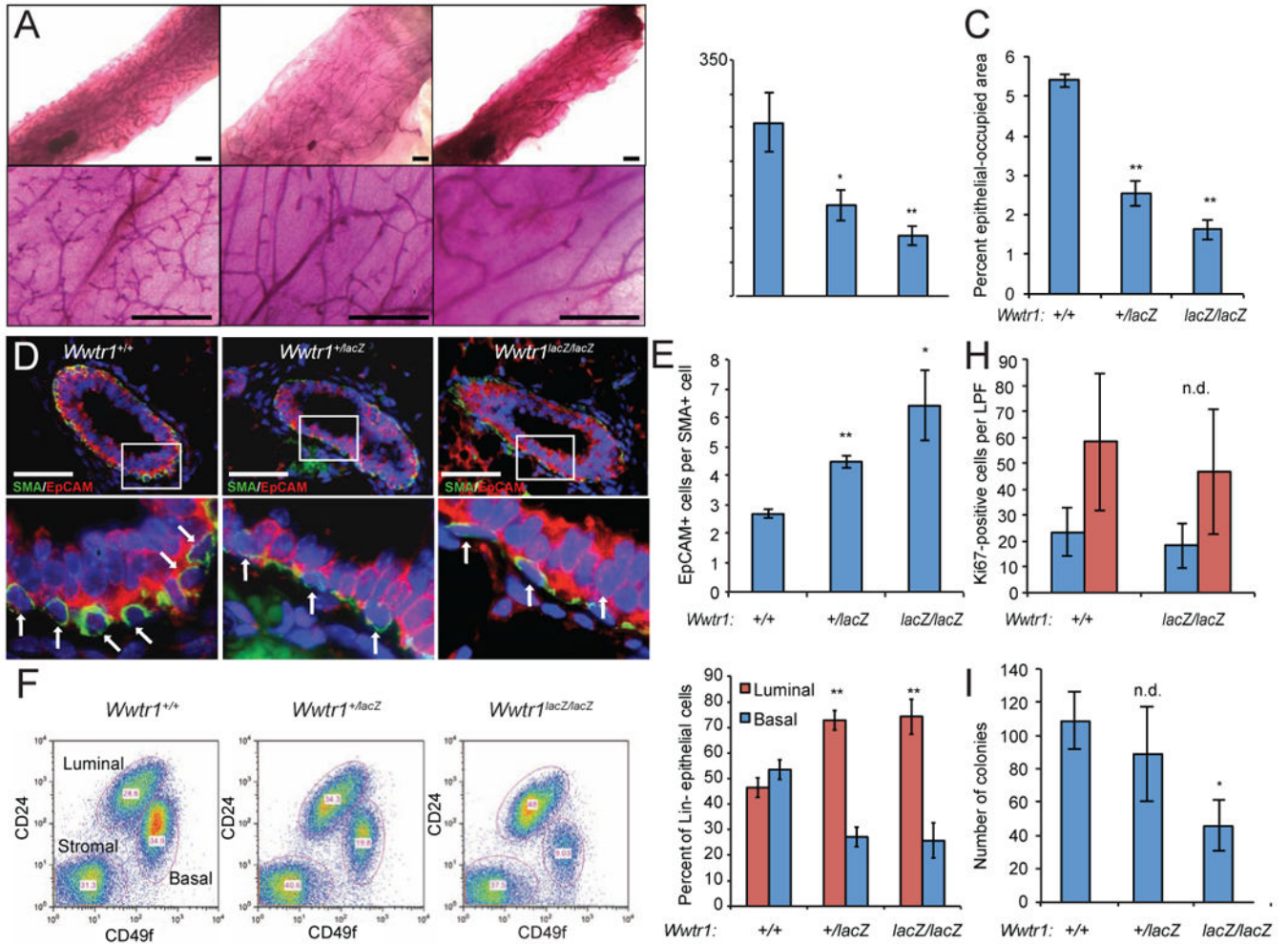
Figure 4. Developmental defects and lineage imbalance in *Taz/Wwtr1*-deficient mice
A, Whole-mount images and **B**, quantification of branching complexity in mammary glands from post-pubertal 16-week old *Wwtr1^lacZ* mice (N = 6 per genotype). **C**, Quantification of the average percentage of cross-sectional gland area occupied by epithelium in 16-week old mice. **D**, Co-immunostaining of epithelia from 16-week old mice for EpCAM (red) and SMA (green) revealed a reduced number of SMA+ cell bodies in *Wwtr1*-deficient glands (arrows in bottom panels, N = 4 per genotype). **E**, Ratio of luminal to basal cells as identified by staining in **D**. **F-G**, MECs were isolated as a single-cell suspension and analyzed by flow cytometry. Representative biaxial plots **(F)** and mean proportions **(G)** of Lin⁻CD24^high/CD49^low luminal and Lin⁻CD24⁺/CD49^high basal cells within *Wwtr1*-deficient epithelia are shown (N = 6 per genotype). **H**, Quantitation of Ki67-positive cells in 16-week old mouse mammary tissues. **I**, Colony formation when MECs from 16-week old mice were plated at clonal density on plastic substrates (N = 3). In all panels, error bars represent SEM, a single asterisk indicates $p < 0.05$ and double asterisks represents $p < 0.01$ as determined by Student's t-test (pairwise against wild-type). See also Figure S3.
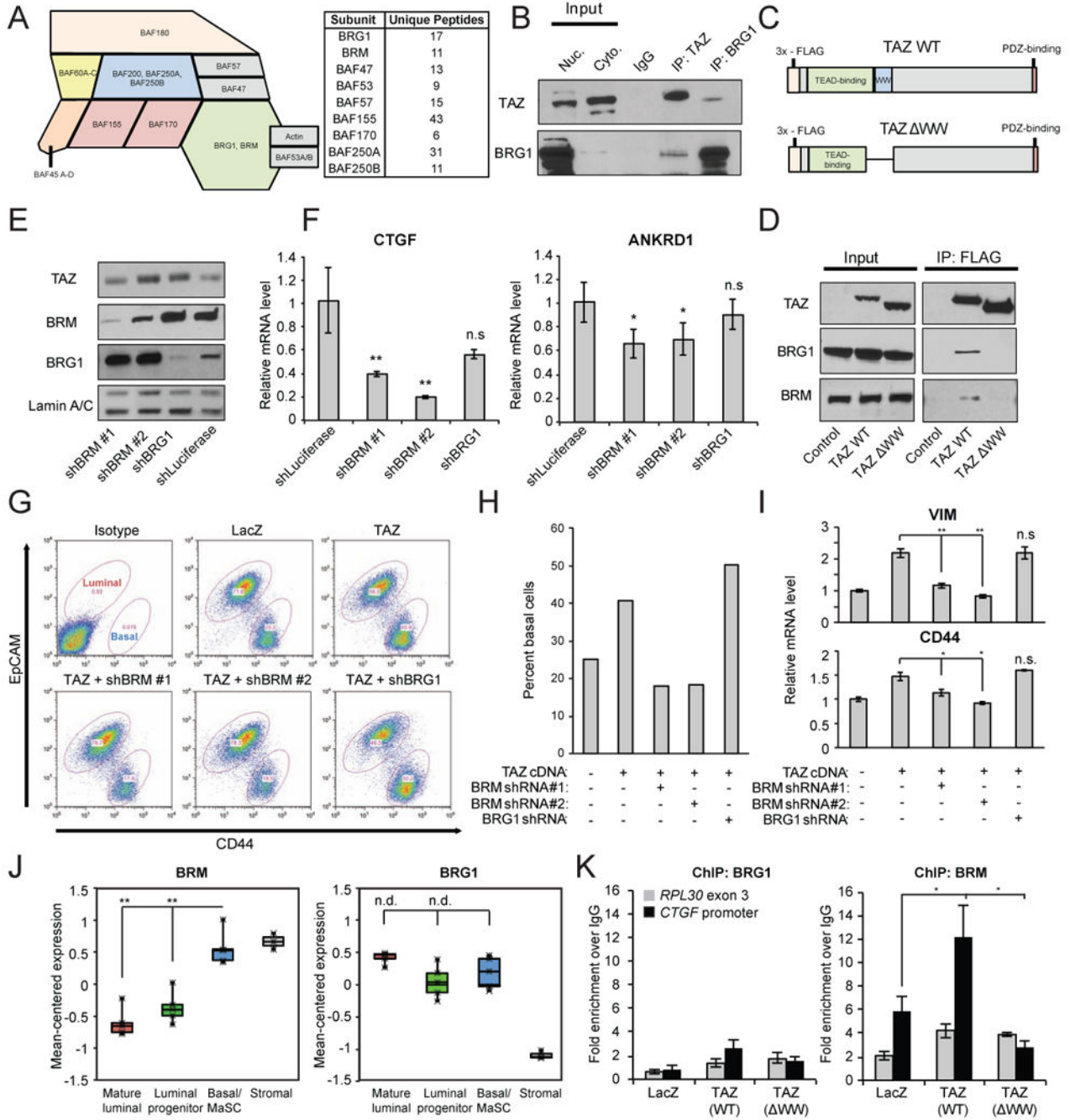
Figure 5. Chromatin-remodeling complexes mediate the function of TAZ
A, Schematic of canonical SWI/SNF subunits (left) with a list of the components identified by TAZ-FLAG co-IP/mass spectrometry (right). **B**, Co-immunoprecipitation of endogenous TAZ and BRG1, one of the two SWI/SNF ATPases, in nuclear lysates from MCF10A cells. **C-D**, FLAG immunoprecipitation of either wild-type TAZ, or a deletion mutant lacking the WW domain,n in 293T cells. **E**, Western blot demonstrating BRM or BRG1 depletion in MCF10F cells using lentiviral shRNA vectors. **F**, qRT-PCR showing the expression of TAZ targets *CTGF* and *ANKRD1* upon BRM/BRG1 knockdown. **G-I**, TAZ cDNA was stably

expressed in MCF10F cells, followed by stable knockdown of BRM or BRG1. **G**, The luminal-like and basal-like MCF10F subpopulations were assessed by flow cytometry and are quantified in **H**. **I**, The expression of basal markers *VIM* and *CD44* was also assessed in MCF10F-TAZ cells with or without BRM or BRG1 knockdown. **J**, Mean-centered gene expression of BRM or BRG1 in mammary epithelial subsets as reported by Lim et al. (2010). **K**, ChIP analysis of BRM and BRG1 at the *CTGF* promoter or *RPL30* exon 3 in MCF10A cells. Data are expressed as a fold enrichment over the IgG negative control. In all panels, error bars indicate SEM, a single asterisk indicates $p < 0.05$ and a double asterisk represents $p < 0.01$ as determined by Student's t-test. See also Figure S4.
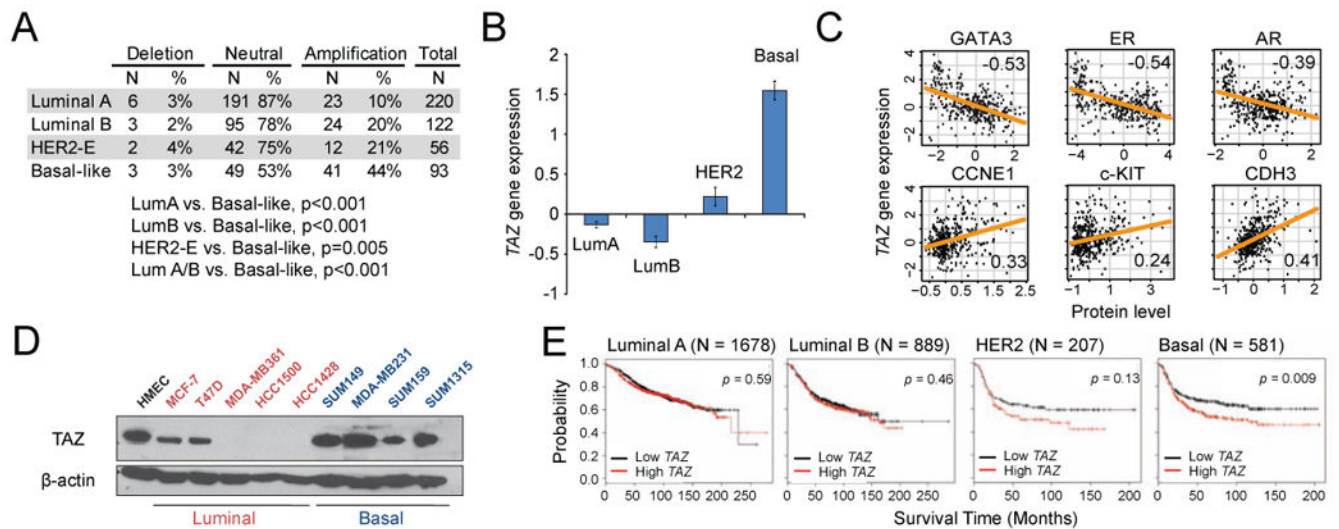
Figure 6. TAZ is associated with basal-like breast cancer
A, Analysis of TCGA data reveals that TAZ copy number is amplified in 44% of basal-like breast tumors (either low- or high-level amplification). **B**, TAZ gene expression is highest in basal-like tumors (error bars indicate SEM). **C**, Correlation between TAZ gene expression and the protein expression of various biomarkers in TCGA dataset (Pearson's R statistic is shown). **D**, Western blot showing TAZ protein levels in various breast cancer cell lines and normal human MECs. **E**, Kaplan-Meier curves showing relapse-free survival probability of patients with high or low TAZ gene expression in various breast cancer subtypes (log-rank p-values are shown).